Int. J. Electrochem. Sci., 10 **(2015)** 848 - 858

International Journal of
ELECTROCHEMICAL
SCIENCE
www.electrochemsci.org

Electrochemical Dissolution of Chalcopyrite Concentrates in Stirred Reactor in the Presence of *Acidithiobacillus ferrooxidans*

Hongbo Zhao[1,2], *Jun Wang*[1,2,*], *Wenqing Qin*[1,2], *Minghao Hu*[1,2], *Guanzhou Qiu*[1,2*]

[1] School of Minerals Processing & Bioengineering, Central South University, Changsha 410083, Hunan, China;
[2] Key Lab of Biohydrometallurgy of Ministry of Education, Changsha 410083, Hunan, China)
[*]E-mail: wjwq2000@126.com; qiuguanzhoucsu@126.com

Received: 24 August 2014 / *Accepted:* 13 October 2014 / *Published:* 2 December 2015

In this work, a new stirred reactor was designed and then a comparative study of bioleaching using stirred reactor and shake flask was carried out to investigate the bioleaching performance of the new stirred reactor. Results showed that variations of redox potentials and acid consumptions during were similar in the two systems, and about 15% more copper extraction can be obtained by stirred reactor. Bacterial concentration increased more sharply in the initial stage of bioleaching in stirred reactor. Analytical results showed that a worse passivation caused by larger amount of jarosite and elemental sulfur on the minerals surface leaded the lower copper extraction in shake flask. Electrochemical analysis revealed that the conductivity of bioleaching residues of shake flasks is lower than that of bioleaching residues of stirred reactor. Stirred reactor possesses significant advantages over shake flask in bioleaching of chalcopyrite concentrates can be caused mainly by better mass transfer effect, better air inflation effect and stronger shear force. Therefore, the stirred reactor can be used for both enlarge cultivation of bacteria and tank bioleaching of ores. Electrochemical measurements revealed that chalcopyrite dissolution was preferred to be a continuous reduction-oxidation pathway, in which chalcopyrite was initially reduced and then oxidized, and the initial reduction reaction was the rate-limiting step.

Keywords: Chalcopyrite concentrates; Electrochemical dissolution; Bioleaching; Stirred reactor

1. INTRODUCTION

Bioleaching remains as a promising technology when compared to the other conventional technologies due to it is considered simple, efficient and eco-friendly. It has shown the potentials to be applied in the processing of copper, nickel, zinc, uranium, refractory gold and other metals, including both dump/heap bioleaching and tank bioleaching processes [1-3]. Tank leaching is commonly used to recover copper from oxidized copper ores and gold from arsenopyrite concentrates, most of the existing commercial plants were for the recovery of gold from arsenopyrite concentrates, while the commercial application of this process for the recovery of copper from concentrates is still in its infancy. This was mainly be attributed to the low leaching rate caused by passivating film on mineral surface, the high cost associated with the manufacture and maintenance, and the loss of microorganism's bioactivity caused by fierce collision and friction [4-6]. Therefore, the reactor is one of the most important factors affecting the tank bioleaching process, and it should be an access to the higher extraction of chalcopyrite concentrates in industry application.

Acidithiobacillus ferrooxidans is one of the most commonly studied bacteria in bioleaching, it is also considered as the dominate population in most acid mine drainage (AMD) as its strong abilities to oxidize ferrous ions and sulfur. Many studies revealed that the mass transfer effect and air inflation effect can significantly affect the efficiency of bioleaching in the presence of *Acidithiobacillus ferrooxidans* [7-9].

Therefore, a new stirred reactor was designed to enhance the bioleaching efficiency, and then a comparative study on bioleaching by this stirred reactor and shake flask was carried out to evaluate the bioleaching performance of the new stirred reactor. Additionally, the electrochemical dissolution process of chalcopyrite was investigated by electrochemical measurements.

2. MATERIALS AND METHODS

2.1 Chalcopyrite concentrates

The chalcopyrite concentrates from Chambishi of Zambia were grinded and sieved to -0.074 mm before bioleaching. X-Ray Diffraction (XRD) analysis showed that chalcopyrite was the main mineralogical composition. Chemical elements analysis showed that the chalcopyrite concentrates mainly contained 30.29% Cu, 19.18% Fe, and 23.6% S (wt%), respectively.

2.2 Microorganisms and culture conditions

Acidithiobacillus ferrooxidans used was obtained from Key Laboratory of Biometallurgy of Ministry of Education, Central South University, Changsha, China. Bacteria were cultured in 250 mL shake flasks using an orbital incubator with a stirring speed of 200 rpm at 30 ^{o}C. The 9K medium used for cell cultivation consisted of the following components: $(NH_4)_2SO_4$ (3.0 g/L), $MgSO_4·7H_2O$ (0.5 g/L), K_2HPO_4 (0.5 g/L), KCl (0.1 g/L), $Ca(NO_3)_2$ (0.01 g/L). These chemicals were added into distilled water, and the pH value was adjusted to 1.6 by sulfuric acid. All the bacterial cultures were sub-cultured into basal salts medium supplemented with 2% chalcopyrite concentrates as the energy source. The resulting culture was used as inoculums for the all bioleaching experiments.

2.3 Bioleaching experiment

2.3.1 Bioleaching in shake flask

One 250 mL shake flask containing 90 mL of 9Kmedium, 5 g chalcopyrite concentrates (5% pulp density), and 10 mL bacterial cultures (10%) was used. The shake flask was placed into an orbital shaker at 200 r/min and 30 ^{o}C, pH value was adjusted to 1.6 regularly, water lost by evaporation was supplemented periodically by adding sterile 9K medium.

2.3.2 Bioleaching in stirred reactor

The system of new stirred reactor was shown in Fig.1, one air pipe connected with air pump was placed into the stirred reactor, fours baffles were fixed on the inner wall, water of 30 ^{o}C was recycled in a interlayer to maintain a constant temperature, sulfuric acid and supplementary 9K medium were added through a pump, pH value and redox potential could be obtained from the microcomputer. The tank bioleaching experiment was conducted in a stirred reactor of 5 L containing 250 mL of bacterial cultures (10%), 2250 mL of 9K medium and 75 g chalcopyrite concentrates (5% pulp density). Stirring rate was adjusted at 200 r/min, the pH value was adjusted to 1.6 by solution of sulfuric acid and sodium hydroxide regularly. During the bioleaching process, record the variation of pH values, bacterial concentration, redox potential and copper concentration regularly.

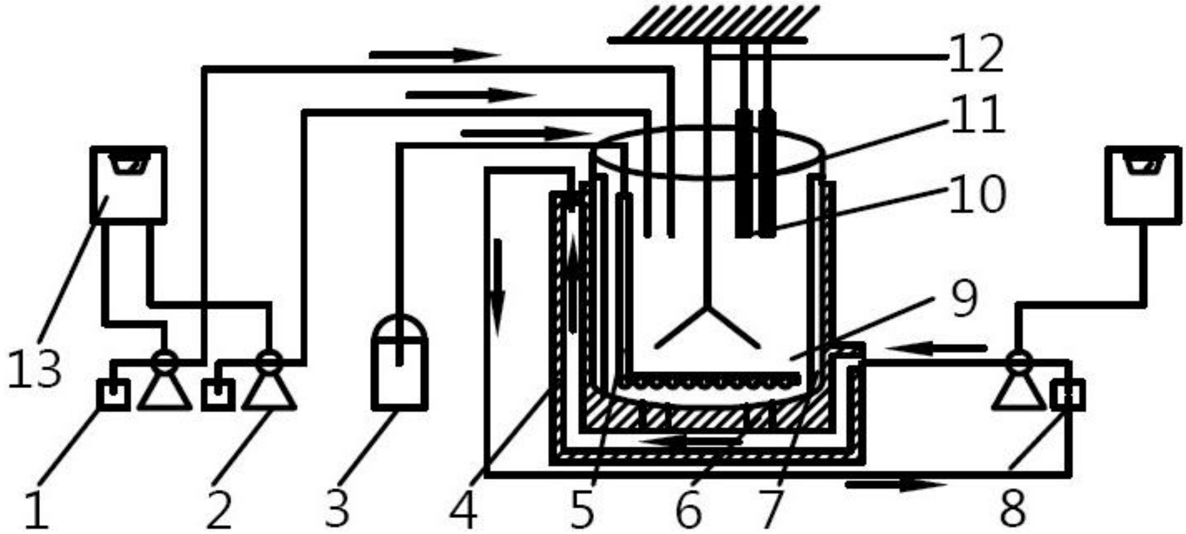

1-Tank; 2-Constant flow pump; 3-Air pump; 4-Insulation sandwich; 5-Air pipe; 6-Reaction tank; 7-Baffle; 8-Thermostatic water bath; 9-Air vent; 10-pH electrode; 11-Eh electrode; 12-Stirring paddle; 13-Microcomputer

Figure 1. The system of new stirred reactor for tank bioleaching

2.4 Electrochemical measurements

2.4.1 Electrodes

The Carbon Paste Electroactive Electrodes (CPEE) were made by mixing 0.7 g minerals (-0.038 mm), 0.2 g graphite and 0.1 g solid paraffin. The mixture was heated and then transferred rapidly into a tablet model for tabletting under the pressure of 500 kg/cm^2, and then took out for air drying. High purity of chalcopyrite sample from Meizhou, Guangdong Province, China, was cut into a cylinder electrode with a diameter of about 1.5 cm, a thickness of about 5 mm, and area of 1 cm^2 of the cylinder surface exposed to the solution. The electrodes were polished using 600-grit metallographic abrasive paper before every electrochemical experiment.

2.4.2 Electrochemical measurements

For all the electrochemical experiments, a conventional three-electrode system consisted of working electrode, graphite rod as counter electrode and Ag/AgCl (3.0 M KCl) electrode as reference electrode was used. The electrolyte was sterile 9K medium with pH value of 1.6. The electrochemical measurements were conducted on a Princeton Model 283 potentiostat (EG&G of Princeton Applied Research) coupled to a personal computer. Cyclic voltammetry tests were carried out at a sweep rate of 25 mV/s, tafel tests were carried out at a sweep rate of 0.5 mV/s, and the potentiostatic tests were all performed under the length of time of 120 s. All potential values in the present work were versus the Ag/AgCl reference electrode (vs. Ag/AgCl).

2.5 Calculation of acid consumption

The consumption of acid was represented by the amount of H$^+$ consumption for per gram of chalcopyrite concentrates each day, it could be calculated by the equation as Eq.(1).

$$N = (10^{-a} - 10^{-b}) \times 1000V / M \qquad (1)$$

Where N is the consumption of H$^+$ for per gram of chalcopyrite concentrates, with unit of mmol/g; a is the pH value measured on former day (measured after adding sulfuric acid), b is the pH value measured on the following day (measured before adding sulfuric acid); V is the total volume of leaching solution, with unit of L; and M is the weight of added chalcopyrite concentrates, with unit of g.

2.6 Analytical techniques

The mineralogical compositions of solid samples were examined by X-ray diffraction (XRD) (DX-2700). Copper concentration was determined by inductively coupled plasma-atomic emission spectrometer (ICP-AES) (America Baird Co. PS-6). The pH values were measured with a pH meter (PHSJ-4A) and the redox potentials of leaching solution were measured by a Pt electrode with reference to a Ag/AgCl electrode (3 M KCl) (BPP-922). Utilize the microscope (Q2270113) to determine the bacterial concentration.

3. RESULTS AND DISCUSSION

3.1 The acid consumptions

The acid consumption everyday was shown in Fig.2 (a). It showed that the trends of acid consumption of bioleaching in stirred reactor and shake flask were similar. It revealed that the first 10 days is a period of acid consumption according to the following chemical reactions of Eq.(2)-Eq.(4) [1, 10].

$$Cu_5FeS_4 + O_2 + 4H^+ \rightarrow 5Cu^{2+} + Fe^{2+} + 2H_2O \quad (2)$$

$$CuFeS_2 + O_2 + 4H^+ \rightarrow xCu^{2+} + yFe^{2+} + Cu_{1-x}Fe_{1-y}S_{2-z} + zS^0 + 2H_2O + 2(x+y)e^- \quad (3)$$

$$4Fe^{2+} + O_2 + 4H^+ \rightarrow 4Fe^{3+} + 2H_2O \quad (4)$$

The amount of acid consumption decreased along with the bioleaching process, this can be mainly attributed to the chemical reactions producing sulfuric acid shown as Eq.(5) [1, 11].

$$2S^0 + 3O_2 + 2H_2O \rightarrow 2SO_4{}^{2-} + 4H^+ \quad (5)$$

3.2 The redox potentials

Fig.2 (b) showed that the variations of potential during bioleaching in stirred reactor and shake flask were similar. As solution potential is mainly determined by c (Fe^{3+})/c (Fe^{2+}) and c (H^+)/(OH^-), therefore, in the initial stage of bioleaching, the redox potential continued to increase due to the above oxidation reactions of ferrous ions to ferric ions (Eq.4). After 15 days of bioleaching, the redox potential reached at a relatively stable value around 600 mV mainly because of the balance between producing and consumption of ferric ions as the formation of jarosite (Eq.6).

$$M^+ + 3Fe^{3+} + 2SO_4{}^{2-} + 6H_2O \rightarrow MFe_3(SO_4)_2(OH)_6 + 6H^+ \quad (6)$$

Where M is a monovalent cation, such as H_3O^+, Na^+, K^+ and NH_4^+, etc.

3.3 The bacterial concentrations

Fig.2 (c) indicated that the variations of bacterial concentration were similar, the bacteria in stirred reactor grew rapidly to logarithmic growth phase without a significant lag phase when compared with the bacteria in shake flask, and the bacterial concentration during the whole bioleaching process in stirred reactor is significantly higher than that in shake flask, revealing that stirred reactor is beneficial to the growth of bacteria during bioleaching, and is able to be applied in large scale cultivation of bacteria.

3.4 The copper extractions

Fig.2 (d) showed that a final copper extraction rate of about 60% can be obtained using stirred reactor, compared with that of about 45% using shake flask, indicating that 15% more copper extraction can be achieved by tank bioleaching in this new stirred reactor. This result definitely demonstrated that the new stirred reactor has significant advantages over shake flask in bioleaching of chalcopyrite concentrates.

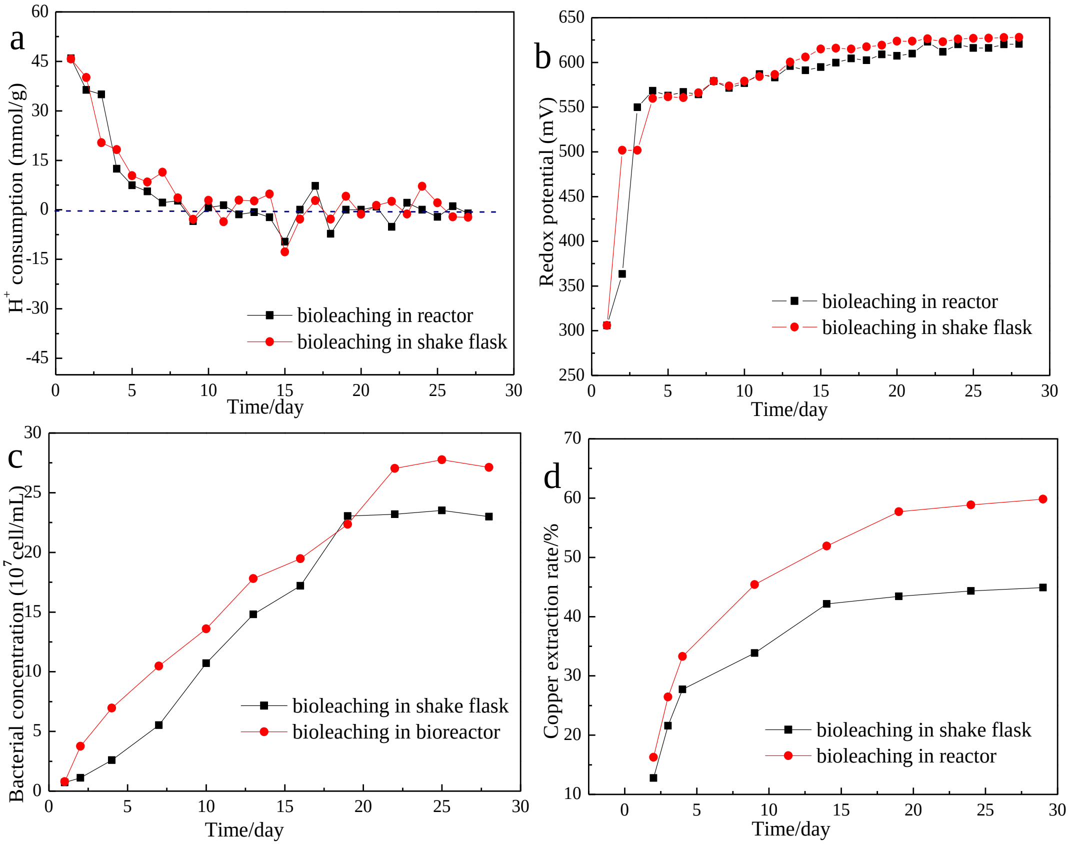

Figure 2. Bioleaching of chalcopyrite concentrates: (a) H^+ consumption for per gram of chalcopyrite concentrates; (b) The variation of redox potential; (c) The variation of bacterial concentration; (d) The copper extraction

3.5 The bioleaching residues

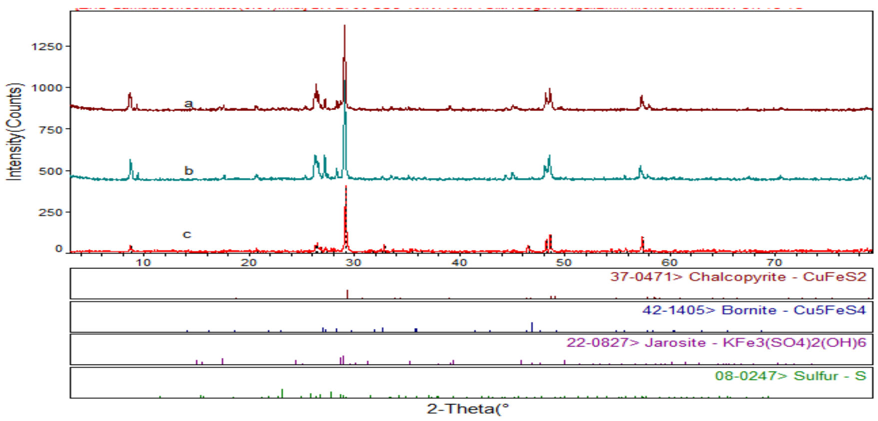

Figure 3. X-ray diffraction (XRD) of bioleaching residues (**a**: bioleaching residue using stirred reactor; **b**: bioleaching residue using shake flask; **c**: chalcopyrite concentrates before bioleaching)

XRD analysis shown in Fig.3 indicated that significant amount of elemental sulfur and jarosite formed on the surfaces of minerals after bioleaching. The amount of jarosite and elemental sulfur formed during bioleaching in shake flask was relatively larger, indicating that the new stirred reactor is beneficial to decreasing the amount of passivation film mainly consisted of jarosite and elemental sulfur.

3.6 The electrochemical measurements of bioleaching residues

3.6.1 Cyclic voltammetry tests

Fig.4 showed the cyclic voltammogram with sweep rate of 25 mV/s, the initial scan was from -0.8 V towards positive direction and then switched at 0.8 V towards negative direction. In the anodic scan from -0.8 V to 0.8 V, four significant anodic peaks were detected of all the three electrodes. Based on the chemical reaction of chalcopyrite to elemental copper (Eq.(7)), the peak a, peak b and peak c can be attributed to the formation and further oxidation of chalcocite (Cu_2S)as reported by many researchers (Eq.(8)-Eq.(10)) [12-14].

$$CuFeS_2 + 4H^+ + 2e^- \rightarrow Cu^0 + 2H_2S + Fe^{2+} \qquad (7)$$

$$2Cu + H_2S \rightarrow Cu_2S + 2H^+ + 2e^- \qquad (8)$$

$$Cu_2S \rightarrow Cu_{2-x}S + xCu^{2+} + 2xe^- \qquad (9)$$

$$Cu_{2-x}S \rightarrow CuS + (1-x)Cu^{2+} + (2-2x)e^- \qquad (10)$$

One anodic peak d can be detected at about 300-600 mV, which was considered as the main range of potential for the decomposition of chalcopyrite and bornite shown as Eq.(11)-Eq.(12) [13, 15, 16].

$$CuFeS_2 \rightarrow xCu^{2+} + yFe^{2+} + Cu_{1-x}Fe_{1-y}S_{2-z} + 2(x+y)e^- \qquad (11)$$

$$Cu_5FeS_4 + 6H^+ \rightarrow CuS + (4-x)Cu^{2+} + 3H_2S + Fe^{3+} + (5-x)e^- \qquad (12)$$

It indicated that the oxidation peaks of both two electrodes of bioleaching residues shifted towards the negative direction in this potential range, it can be because of the decomposition of chalcopyrite and bornite to Cu-Fe-S intermediate species, of which the oxidation potential was lower.

In the cathodic scan from 0.8 V to -0.8 V, two obvious peaks were observed, peak e can represent the reduction of ferric ions, copper ions and elemental sulfur shown as Eq.(13)-Eq.(15) [17-19].

$$Fe^{3+} + e^- \rightarrow Fe^{2+} \qquad (13)$$

$$Cu^{2+} + S^0 + 2e^- \rightarrow CuS \qquad (14)$$

$$Cu^{2+} + 2e^- \rightarrow Cu^0 \qquad (15)$$

Peak f can be associated with the formation of chalcocite and its further reduction to elemental copper shown as Eq.(16)-Eq.(18) [16, 18, 20]. It revealed that the electrodes of bioleaching residues were prone to be reduced to chacocite.

$$2CuS + 2H^+ + 2e^- \rightarrow Cu_2S + H_2S \qquad (16)$$

$$2CuFeS_2 + 6H^+ + 2e^- \rightarrow Cu_2S + 2Fe^{2+} + 3H_2S \qquad (17)$$

$$Cu_2S + H^+ + 2e^- \rightarrow 2Cu^0 + HS^- \qquad (18)$$

The cyclic voltammogram curves of the two electrodes of bioleaching residues were similar. However, the current densities during anodic scan were significantly different, especially in the potential range of about 300-600 mV, the current density of residue from shake flask was lower than that of residue from stirred reactor, indicating a lower oxidation rate of residue from shake flask. This can mainly be attributed to a worse passivation of chalcopyrite concentrates during bioleaching in shake flask.

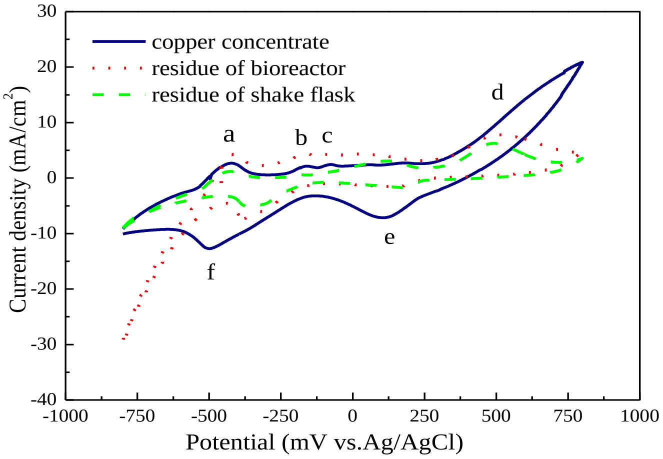

Figure 4. Cycle voltammograms of chalcopyrite concentrates and bioleaching residues

3.6.2 Tafel tests

Fig.5 showed the tafel curves of chalcopyrite concentrates and bioleaching residues, the corresponding parameters of corrosion potential (E_{corr}), corrosion current density (i_{corr}) and polarization resistance (R_p) were calculated.

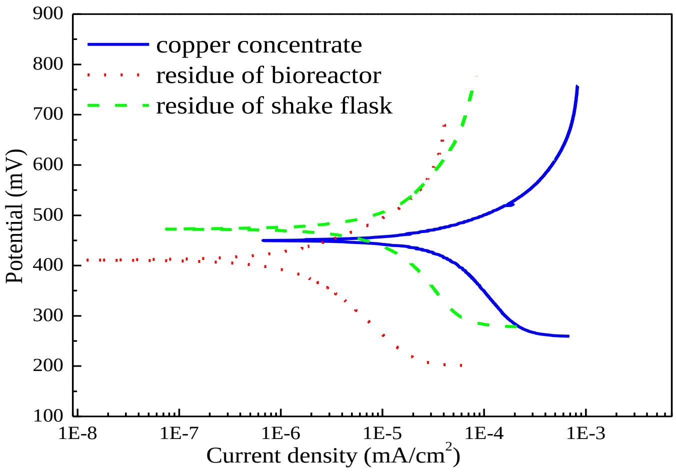

Figure 5. Polarization curves of chalcopyrite concentrates and bioleaching residues

The corrosion potential of chalcopyrite concentrates, residue of stirred reactor and residue of shake flask were 449.8 mV, 410.9 mV and 472.7 mV, the corresponding corrosion current density of these three samples were 206.1 µA/cm^2, 5.581 µA/cm^2 and 1.237 µA/cm^2, the polarization resistance (R_p) were 0.678 KΩ•cm^2, 14.3 KΩ•cm^2 and 3500 KΩ•cm^2, respectively. The lowest corrosion current density and the largest polarization resistance were obtained from the residue of bioleaching in shake flask because of its worse passivation, and this was consistent with the analytical results above.

3.7 Investigation of electrochemical dissolution process of chalcopyrite

3.7.1 Cyclic voltammetry tests

Fig.6 showed the cyclic voltammograms of chalcopyrite electrode in two different scan routes. The positive scan route started scanning from 0.3 V towards anodic direction, then reversed to cathodic direction, and finally switched towards anodic direction again. The negative scan route started scanning from 0.3 V towards cathodic direction, then switched towards anodic direction, and finally reversed to cathodic direction. Higher current density of peak 1 during negative scan route can be detected. Peak 1 was in the potential range of about 0.3 V to 0.8 V, where the main oxidation reactions of releasing copper ions took place, indicating that the dissolution of chalcopyrite can be significantly accelerated by the reduction of chalcopyrite.

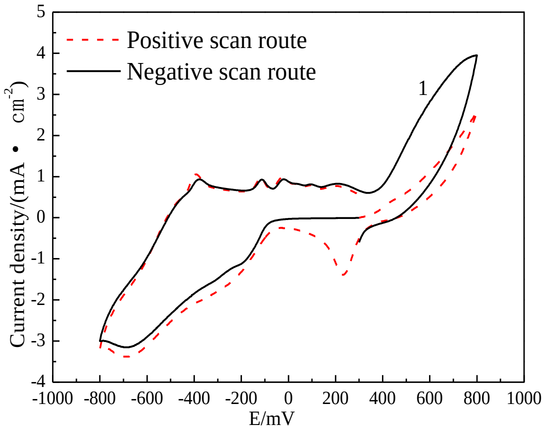

Figure 6. Cyclic voltammograms of chalcopyrite electrode in different scan routes

3.7.2. Potentiostatic tests

To characterize the potential range where oxidation and reduction reactions of dissolution process took place, potentiostatic oxidation and reduction experiments were performed in different potential ranges. The relationship between the total charges (evaluated from the current–time curves of chalcopyrite electrode) and applied potential was shown in Fig.7, which indicated that three different regions existed from -0.6 V to 0.7 V, the smallest slop in the region I (0~0.4 V) suggested that the reactions in this potential range should be the main rate-limiting step during chalcopyrite dissolution process. Therefore, the reduction of chalcopyrite in the initial stage of bioleaching can be the main rate-limiting step.

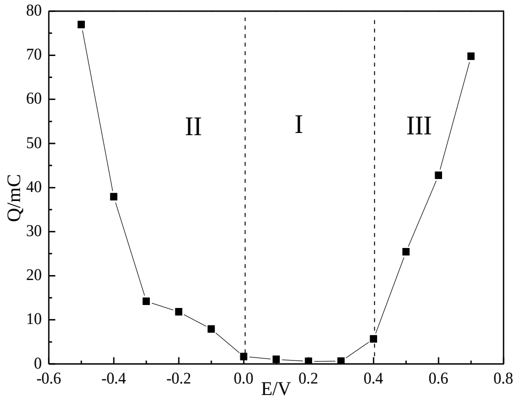

Figure 7. Relationship between the total charges and applied potential pulse

4. CONCLUSIONS

(1) A significantly higher copper extraction of chalcopyrite concentrates bioleaching can be obtained using stirred reactor when compared with that of bioleaching using shake flask.

(2) The chosen stirred reactor is beneficial to the growth of bacteria in the initial stage of bioleaching process, and for decreasing the amount of passivation film mainly consisted of jarosite and elemental sulfur in the later stage of bioleaching as its advantages of better mass transfer effect, better air inflation effect and stronger shear force over shake flask.

(3) Chalcopyrite dissolution was preferred to be a continuous reduction-oxidation pathway, in which chalcopyrite was initially reduced and then oxidized, and the initial reduction reaction was the rate-limiting step.

ACKNOWLEDGMENTS
This work was supported by the National Natural Science Foundation of China (project No. 51374248), Program for New Century Excellent Talents in University (project No.NCET-13-0595), Hunan Provincial Innovation Foundation for Postgraduate (project No. CX2014B091) and China Postdoctoral Science Foundation (project No. 2014T70692).

References

1. H. Watling, *Hydrometallurgy*, 84 (2006) 81.
2. A. Pathak, M. Dastidar, and T. Sreekrishnan, *Journal of environmental management*, 90 (2009) 2343.
3. J. Brierley and C. Brierley, *Hydrometallurgy*, 59 (2001) 233.
4. F. Acevedo, *Electronic journal of biotechnology*, 3 (2000) 10.

5. D. Mishra, D.-J. Kim, J.-G. Ahn, and Y.-H. Rhee, *Metals and Materials International*, 11 (2005) 249.
6. J. Jin, S. Shi, G. Liu, Q. Zhang, and W. Cong, *Minerals Engineering*, 39 (2012) 19.
7. R. E. Mielke, D. L. Pace, T. Porter, and G. Southam, *Geobiology*, 1 (2003) 81.
8. L. Xia, C. Yin, S. Dai, G. Qiu, X. Chen, and J. Liu, *Journal of Industrial Microbiology & Biotechnology*, 37 (2010) 289.
9. Y. Yang, M. Diao, K. Liu, L. Qian, A. V. Nguyen, and G. Qiu, *Hydrometallurgy*, 131 (2013) 93.
10. Y. Li, N. Kawashima, J. Li, A. Chandra, and A. Gerson, *Advances in Colloid and Interface Science*, 197 (2013) 1.
11. B. Fu, H. Zhou, R. Zhang, and G. Qiu, *International Biodeterioration & Biodegradation*, 62 (2008) 109.
12. A. Elsherief, *Minerals Engineering*, 15 (2002) 215.
13. E. M. Arce and I. González, *International Journal of Mineral Processing*, 67 (2002) 17.
14. D. Nava and I. González, *Electrochimica Acta*, 51 (2006) 5295.
15. T. Biegler and D. Swift, *Journal of Applied Electrochemistry*, 9 (1979) 545.
16. G. Gu, K. Hu, X. Zhang, X. Xiong, and H. Yang, *Electrochimica Acta*, 103 (2013) 50.
17. A. Li and S. Huang, *Minerals engineering*, 24 (2011) 1520.
18. C.L. Liang, J.L. Xia, Y. Yang, Z.Y. Nie, X.J. Zhao, L. Zheng, C.Y. Ma, and Y.D. Zhao, *Hydrometallurgy*, 107 (2011) 13.
19. J. Wang, H. Zhao, W. Qin, C. Yang, and G. Qiu, *Int. J. Electrochem. Sci*, 8 (2013) 12590.
20. H. Zhao, J. Wang, M. Hu, W. Qin, Y. Zhang, and G. Qiu, *Bioresource Technology*, 149 (2013) 71.